Research Square

Preprints are preliminary reports that have not undergone peer review.
They should not be considered conclusive, used to inform clinical practice,
or referenced by the media as validated information.

Engineering ZIF-8 morphology for uptake of methomyl residues from wastewater by combining it with extracted lignin as an antibacterial

Reda Abdelhameed
Mohamed Hasanin
Hassan Abdel-Gawad (abdelgawadhassan@hotmail.com)
https://orcid.org/0000-0002-6166-1342
Bahira Hegazi

Research Article

Keywords: Lignin, ZIF-8, Methomyl, Adsorption, H-Bonding mechanism

Posted Date: April 25th, 2022

DOI: https://doi.org/10.21203/rs.3.rs-1573288/v1

License: This work is licensed under a Creative Commons Attribution 4.0 International License.
Read Full License

Abstract

It is highly favorite to remove hazardous substances from insecticides by means of adsorbents with high adsorption uptake. Here, the hybridization between lignin and ZIF-8 and the removal of methomyl insecticides from wastewater were studied. The compounds were assured by FTIR, SEM, XRD, and BET analyses. The effect of some variables such as adsorbent dose and contact time on methomyl removal efficiency was investigated. The reaction mechanism was carefully scanned by SEM and FTIR. Kinetic and isometric parameters have been accurately matched with Langmuir models and pseudo-second-order models. The adsorption capacities in 60% ZIF-8@Lignin approached as high as 324.6 mg g^{-1} which were much higher than Lignin alone. Compared to other works, the present work demonstrated better absorption capacity and cost-effectiveness. Antimicrobial testing approved that addition of ZIF-8 to lignin enhanced microbial activity and the MIC value. The lowest values against all tested microbial strains were 19 mg/mL.

Introduction

Pesticides, in general, are chemicals used worldwide in agricultural production to destroy or control weeds, insects, fungi, and other pests. Nowadays, approximately 1,000 different pesticides are recognized worldwide. Plants were sprayed with large amounts of pesticides, and almost 95% of the pesticides sprayed fell on the soil, where they may pose high risks to both humans and the environment [1].

Among the sprayed pesticides, organophosphates and carbamates account for a large amount of pesticides used due to their low stability and high insecticidal activity. The methomyl insecticide proved as a hazard chemicals from Environmental Protection Agency (EPA), its chemical name *S*-methyl *N*-methyl carbamoyloxy thioacetimidate, (CAS, 16752-77-5) (Fig. 1). Methomyl is widely used as an oxycarbamate insecticide to control many insects to increase crop yield. Considered as one of the highly toxic pesticides, methomyl is introduced into aquatic systems by agricultural activities [2].

Lignin accounts for most of the biomass content, and it is a huge waste in the paper industry [3]. Lignin has the advantages of being environmentally friendly, having abundant reserves, being biodegradable, and being utilized in the fields of thermoplastic materials [4], pesticides[5]. The advantage of lignin lies in its various functional groups that can be used as adsorbents. The disadvantage of lignin is limitation of anion adsorption because of its electronegative functional groups [6]. Moreover, the aqueous lignin solution denatures its application in adsorption [7]. Therefore, lignin modification is necessary for methomyl uptake applications. Removing pesticide residues from wastewater is vital and challenging. Recently, wastewater treatment become the most achievement field and a lot of technologies were applied to uptake dyes, pharmaceutical intermediates and pesticide residues from wastewater, the most traditional technologies are photocatalytic degradation using semi-conducting materials, extraction with solvent, bio-degradation using enzymes and advanced oxidation using ozone and H_2O_2. The disadvantages of these technologies are limitations of degradation capacity, high costs of catalyst production, toxic by-product, and difficulty of separating the catalysts. In comparison, adsorption

represented the most economical method for removal of pesticides; the challenge of this technique is searching about highly adsorbed materials, by getting the suitable and selective adsorbent materials, the adsorption techniques become a promising technologies in removal of pesticides.

Metal organic frameworks (MOFs) represented the most suitable materials for adsorption of pesticides from wastewater because of high surface area, pore size modification and free active sites in the frameworks [8]. Among MOFs used for removal of pesticide from wastewater was MIL-53(Cr), it was used to adsorb 2,4-dichlorophenoxyacetic acid (2,4-D) pesticide with high adsorption capacity (556 mg g^{-1}) [9]. Moreover, the highly toxic ethion was uptake using Cu-BTC with adsorption capacity of ~ 122 mg g^{-1} [10]. The adsorption capacity reached 367 and 279 mg g^{-1} when ZIFs MOFs were used for removal of prothiofos and ethion from wastewater, respectively [11]. The high adsorption capacity appeared when UiO-66(Zr) was used to remove metrifonate and dichlorvos, the maximum adsorption were recorded 379 and 571 mg g^{-1} for metrifonate and dichlorvos, respectively [12]. Recently, the role of amino-doped Al-MOFs was investigated to remove dimethoate from wastewater, the maximum adsorption capacity reached 513.4 mg g^{-1} represented the high add values of amino groups in the framework [13]. Much work was done for enhancement the pesticide adsorption capacity and large scale application via using MOF composites for adsorption of pesticides; ethion was adsorbed onto Cu-BTC@cotton composite with capacity 182 mg g^{-1} [14]. Azole fungicides were removed using Fe_3O_4@ZnAl-LDH@MIL-53(Al) with adsorption capacity 71.79 mg g^{-1}[15]. MOFs was decorated with magnetic nanoparticles (Fe_3O_4) and good hosting material (β-CD) to produce Fe_3O_4@MIL-100(Fe)/β-CD, this material was used to remove triazole fungicides from wastewater with a maximum absorption of 102.10 mg g^{-1} [16]. A short time ago, dimethoate was adsorbed from wastewater with Cu-BTC@Cellulose acetate and the absorption capacity reached 321.9 mg g^{-1} [17]. Chlorpyrifos was adsorbed onto MIL-53-NH_2@CA membrane with 356 mg g^{-1} capacity [18].

Taking into account the advantages of both lignin and MOFs, here, the hybridization of MOFs on lignin was investigated using an easy and high yield method. The role of lignin in the synthesis of the compound (ZIF-8@lignin) as a control factor was studied. Extensive characterization methods were used to determine the effect of lignin on the preparation of ZIF-8@lignin. The adsorption performance of Lignin, 20% ZIF-8@Lignin, 40% ZIF-8@Lignin and 60% ZIF-8@Lignin on removal of methomyl insecticide were extensively investigated.

Material And Methods

Materials

2-Methylimidazole (Hmim), Zinc nitrate [$Zn(NO_3)_2$], methyl alcohol, hydrochloric acid (HCl), sodium hydroxide (NaOH) and all other chemicals were analytical grade reagent and bought from Sigma.

Synthesis of pure methomyl

Methomyl was synthesized according to known method by the condensation reaction of equimoler amounts of *S*-methyl-*N*-hydroxythioacetimidate (0.007 mole, 0.7 g) in methylene chloride with methyl isocyanate (0.007 mole, 0.42 ml) at 30-50°C. It is a white crystalline solid with melting point 77-79°C after recrystalization from benzene (Fig.1). TLC gave on spot using the following solvent systems, System 1: benzene: ethyl acetate, (6: 4 v/v), R_F 0.42, System 2: benzene: methanol: acetic acid (8: 2: 0.1v/v/v), R_F 0.6, respectively, Wave length λ at 233-234 nm. The concentration of methomyl was followed by measuring the absorption of the solution at 233.8 nm, using UV-vis Shimadzu model 1700 spectrophotometer.

Extraction of Lignin

Citrus trees terminal fibers were grinding as subjected to extract lignin. The fibers pulping process was carried out using 17.5 % NaOH at 120°C for 2 h. The silica was extracted from the black liquid according to Minu *et al* [19]. The black liquor pH was adjusted between 6 - 7 using 1M H_2SO_4 and 1M NaOH. The black liquor constancy changed to gel. This is confirming the precipitation of silica. The gel was extracted via vacuum filtration then washing for several times with hot distilled water until the gel color became white. The filter was collected and the pH was set at 2. The precipitate was filtrated and washing for several time by hot distal water and dried in vacuum oven at 70°C [20].

Preparation of ZIF-8@Lignin

ZIF-8@Lignin composites were synthesized as follow: 2-Methylimidazole (Hmim, 4.10 g, 50 mmol) was dissolved in methanol (100 mL) and added a 100 mL of aqueous solution which contained 0.1-0.6 g of lignin. After that, the mixture was stirred continuously for 1 h and ultrasonic treatment for 10 min. The methanol solution of $Zn(NO_3)_2 \cdot 6H_2O$ (2.97 g, 10 mmol) was added into a methanol solution of 2-methylimidazole containing lignin. The mixture was stand with continuous stirring at room temperature for 24 hours. The final solids were separated by centrifugation, washed with methanol and deionized water and dried under reduced pressure for 24 h at 60°C.

Characterization

Fourier transform infrared (FT-IR) spectroscopies of the samples were recorded on a spectrum 100 FT-IR spectrophotometer (Perkin-Elmer, USA) using a KBr disk method and scanned in the range of 4000-450 cm^{-1}. Scanning electron microscopy (SEM) images were examined using a JSM-6700F scanning electron microscope (JEOL Ltd., Japan). The specific surface area and pore size of the adsorbents were measured at 77 K (the boiling point of nitrogen) with the help of a volumetric adsorption analyzer (ASAP 2420, Micrometrics, USA). The Brunauer-Emmett-Teller (BET) and Barrett-Joyner-Halenda (BJH) techniques were used to determine the area and calculate the pore size. Powder XRD data were collected on a PANalytical X'Pert PRO diffractometer with Cu Kα radiation as the X-ray source. The pesticide content of the test samples was analyzed using a Shimadzu UV-vis spectrophotometer model 1700.

Adsorption experiments

The insecticide methomyl was used to examine the adsorption capacity of the prepared products. Adsorption experiments were conducted by adding a certain amount of adsorbents to a certain volume of methomyl solutions under continuous stirring at room temperature, for example, 50 mg of Lignin, 20% ZIF-8@Lignin, 40% ZIF-8@Lignin and 60%ZIF-8@Lignin were added to 50 mL of methomyl solution. Adsorption isotherms experiments were carried out at different methomyl concentrations (25-1000 mg L^{-1}, 50 mL) with 25 mg of Lignin, 20% ZIF-8@Lignin, 40% ZIF-8@Lignin and 60% ZIF-8@Lignin at pH 7 for 24 h. Adsorption kinetics were studied by adding 50 mg of adsorbent into 25 mL of 100 mg L^{-1} methomyl solution. The samples were obtained at given intervals and examined using UV-Vis spectrophotometer at 233.8 nm for methomyl. The adsorption amount (q, mg g^{-1}) was calculated as follow:

$q=(c_0-c)\times Vm$, $q=(c_0-c)\times Vm$,

Where V (L) is the solution volume, m (g) is the adsorbent mass, and c_0 (mg L^{-1}) and c (mg L^{-1}) are the initial and final concentrations of pesticide, respectively.

Microbial strains

Cultures of the following microorganisms were used in the tests: (i) Gram-negative bacteria: *Escherichia coli* (*NCTC-10416*), (ii) Gram-positive bacteria: *Staphylococcus aureus* (*NCTC-7447*) and, (iii) unicellular fungi: namely, *Candida albicans* (NCCLS 11) by using nutrient broth medium.

Antimicrobial study

The antimicrobial test of tested samples was carried out using 0.5g following the cell formation unite counting (CFU) technique as described in our previous work [21-23]. Minimal inhibition concentration (MIC) was calculated for the crude antimicrobial material according to Balouiri method [24] using serial dilution method via turbid metric technique. Streptomycin and Griseofulvin antibiotics were used as reference in antibacterial and antifungal tests.

Results And Discussion

The physical properties of MOFs can be changed without the need to change the chemical structure, just change the morphology with MOF nanocrystals assembled into well-ordered superstructures. Here ZIF-8 nanorods are assembled through interfacial synthesis templates by adding an amount of lignin in a synthetic procedure bath. Figure 1 depicts the chemical composition of the prepared materials.

Characterization of adsorbents

The morphology and particle size of the prepared products were studied by SEM analysis, as shown in Figure 2. The prepared 60% ZIF-8@Lignin crystals exhibit rode shape, it is completely different than ZIF-8

alone that is typical rhombic dodecahedral structure. The particle sizes and distribution of 60%ZIF-8@Lignin composites are slightly influenced by the lignin addition.

The FTIR spectrum of Liginin, ZIF-8, 20% ZIF-8@Lignin, 40% ZIF-8@Lignin and 60% ZIF-8@Lignin are shown in Figure 3. The main characteristic absorption peaks for all formulated materials (ZIF-8 and ZIF-8 @Lignin) are compatible with previous research [11, 25, 26]. The imidazole ring out of plan transmission peaks is ascribed to the range 500-820 cm^{-1}, whereas the in-plane is attributed to the range 890-1340 cm^{-1}. The imidazole ring vibration is correlated with the areas 1340–1550 cm^{-1}, and the C = N stretch is correlated with the adsorption band at 1578 cm^{-1}. The -OH groups of lignin and the adsorption band at around 3430 $cm^{-1}$are connected at 3132 cm^{-1} and 2927 cm^{-1}, the C–H stretching of the 2-methylimidazole ring and the aliphatic chain are exhibited, respectively. Peaks at 2900 cm^{-1} correspond to the vibration of the C–H bond in methyl groups ($-CH_3$) of liginin molecule. Moreover, liginin molecules showed peaks at 1700-1660 cm^{-1} correspond to carbonyl bond vibrations in carboxylic group, also it exhibited peaks at 1500-1600 cm^{-1} related to aromatic ring vibrations and C–H, O–H, C=O bonds. Additionally, peaks at 1460 cm^{-1} correspond to methyl group C–H bonds and peaks at 1420 cm^{-1} correspond to aromatic ring vibrations of liginin molecules. A comparison of the ZIF-8 and ZIF@Lignin compounds demonstrates a difference, particularly the peaks at 422, 672, and 745 cm^{-1} bound to the Zn-N, C=N, and imidazole rings, respectively.

Figure 4 displays the XRD pattern of the prepared products. The XRD pattern of ZIF-8 is consistent with previous reports [12, 27], indicating that ZIF-8 nanocrystals have been successfully synthesized. Lignin shows the maximum 2θ values at 20.26 and 22.94 confirming successful extraction of lignin from citrus materials [25]. The XRD patterns of ZIF@lignin compounds include peaks for both ZIF-8 and lignin. The high sharpness and intensity of their XRD patterns indicate the high crystallinity of ZIF@Lignin compounds, indicating that ZIF-8 nanocrystals were successfully grown in lignin solution during in situ synthesis and incorporation of lignin did not destroy the framework integrity of ZIF-8.

Adsorption isotherms for methomyl removal

To study the adsorption performance and mechanism, Langmuir and Freundlich isothermal models are used to analyze the adsorption data. Theoretical Langmuir is one of the most traditional isoform. It has a maximum adsorption capacity to form a monolayer on the outer surface of the absorbent material which is calculated according to the formula and is expressed as:

$C_eQ_e=C_eQ_m+1K_LQ_m$

where Q_e is the amount of methomyl insecticide per gram of the adsorbent at equilibrium (mg g^{-1}), C_e is Equilibrium concentration of adsorbate (mg L 1), Qm refers to the maximum coverage capacity of the monolayer (mg g-1), KL is the isothermal Langmuir constant (L mg-1) which relates to the adsorption energy and the affinity of the binding sites. The indicated adsorption isotherms with a heterogeneous and

multilayered surface are described by the Freundlich model. This form can be calculated according to the equation which is expressed as:

$Q_e=K_fC_e1/n$

Kf shows information about the bonding energy known as the adsorption coefficient or distribution (mg g 1) and represents the amount of carbamate adsorbed on the sorbent. 1/n shows the adsorption density of the insecticides on the adsorbents.

Adsorption isotherms for methomyl were determined on, ZIF-8, 20% ZIF-8 @Lignin, 40% ZIF-8 @Lignin and 60% ZIF-8 @Lignin at room temperature (25 °C) after sufficiently adsorbed duration 210 minutes. Adsorption capacities increase with increasing initial pesticide concentration (Figure 5). The adsorption coefficients are shown in Table 1.

Table 1. Parameters of isotherm for adsorption of Methomyl onto Lignin, and ZIF-8@Lignin (20, 40 and 60%)

Samples	Freundlich parameters				Langmuir parameters			
	n	K_F	R^2	$\chi2$	Q_m (mg g^{-1})	K_L	R^2	$\chi2$
Lignin	2.76 ±0.35	9.72 ±2.75	0.977	35.13	130.2 ±2.66	0.005 ±3.75	0.997	3.11
20%ZIF-8@Lignin	3.03 ±0.28	17.41 ±3.18	0.987	37.87	168.4 ±6.76	0.009 ±0.001	0.989	30.1
40%ZIF-8@Lignin	3.26 ±0.68	28.65 ±10.4	0.930	375.1	220.6 ±8.59	0.013 ±0.001	0.989	58.5
60%ZIF-8@Lignin	2.51 ±0.37	25.71 ±7.97	0.956	419.4	324.6 ±10.38	0.011 ±0.001	0.995	41.2

Effect of contact time

The adsorption behavior of methomyl over time from aqueous solution to Lignin, 20% ZIF-8 @Lignin, 40% ZIF-8 @Lignin, and 60% ZIF-8 @Lignin is represented in Figure 6. As can be seen for Lignin, 20%ZIF-8@Lignin, 40%ZIF-8@Lignin and 60%ZIF-8@Lignin the adsorption capacities for methomyl insecticides increase quickly during the first 90 min and reach equilibrium in 3hours. Due to the abundance of vacant adsorption sites available at the beginning of the adsorption process, rapid removal of the insecticides can be observed. The available sites become less after a period of time, so it gradually decreases at a higher conversion uptake rate. Furthermore, the cavities in the MOFs might be partially blocked by

methomyl molecules, which also have a negative impact on the adsorption rate. The kinetic parameters were seen in table (2).

Table 2. Parameters of adsorption kinetics of methomyl onto Lignin, and ZIF-8@Lignin (20, 40 and 60%)

Samples	Q_e exp.	pseudo-first-order parameters				pseudo-second-order parameters			
		Q_e	K_1	R^2	χ^2	Q_e	$K_{2*}10^{-4}$	R^2	χ^2
Lignin	85.8	81.066 ±1.65	0.024 ±0.002	0.991	8.20	93.39 ±2.72	3.22 ±5.004	0.992	7.05
20%ZIF-8@Lignin	114	107.5 ±2.97	0.019 ±0.002	0.986	21.5	127.8 ±2.64	1.71 ±1.67	0.997	4.79
40%ZIF-8@Lignin	150	144.3 ±4.19	0.0145 ±0.001	0.989	30.6	178.49±4.34	8.69 ±8.84	0.997	8.28
60%ZIF-8@Lignin	168	171.7 ±2.69	0.015 ±8.45	0.996	13.5	211.71±11.4	7.50 ±1.70	0.985	59.05

Mechanism of methomyl adsorption

Methomyl is a polar insecticide containing functional groups like C=O that can engage H bonds, and the presence of a C=O bond causes the methomyl structure to be highly polar. [27]. The most abundant biopolymer is lignin, which is generated from plant sources during cellulose production. Synthetic lignin is typically produced as a by-product or waste during the biofuel and pulp manufacturing processes. Lignin is an aromatic three-dimensional structure with a large number of phenolic, hydroxyl, carboxyl, methoxy, and aldehyde functional groups. These lignin functional groups may have an affinity for methomyl absorption throw hydrogen bonding mechanism (Figure 7).

As can be shown in Figure 8, the morphology of the particle before and after adsorption was determined using SEM. The microscopic images show that the crystal size is the same after adsorption of carbamates. Small aggregation of MOFs was seen in SEM image, however, no clear differences in the morphologies observed. EDX (Fig 8 c and d) show important notification, sulphur element was appeared in EDX mapping confirming the presence of methomyl insecticide in the composite.

Methomyl adsorption was determined using FTIR spectra. Both lignin and ZIF-8@Lignin after adsorption of methomyl are depicted in Figure 9. Peak at 1601 cm^{-1} was appeared in FTIR spectrum because of primary amines [28]. Additionally, the peak at 1706 cm^{-1} was appeared in the lignin structure after

adsorption due to the presence of C=O bond of methomyl. For ZIF-8@Lignin, both peaks at 2116 cm^{-1} and 1391 cm^{-1} were disappeared. This indicates the absence of –C≡C– stretch of alkyne groups and absence of C-C stretch (in- ring) of aromatic rings, respectively. Also, new peak appeared at 1601 cm^{-1} due to NH bond which indicates the presence of methomyl in the composite after adsorption [28].

A compassion between pervious literature for methomyl removal from wastewater and the present work (60% ZIF-8@Lignin) were shown in Table 3. It is shown that 60% ZIF-8@Lignin has 8 times higher than hyper cross linked polymers, but it has 2.6 times higher than nanoporous activated carbon xerogels.

Table 3. Comparison of adsorption capacities of methomyl on different adsorbs

Adsorbents	Q mg/g	References
Hypercrosslinked polymers Macronet MN-150	40	[29]
Natural clay	0.539	[30]
Cotton stalks activated carbon	72.85	[31]
Nanoporous activated carbon xerogels	125	[32]
Hypercrosslinked polymer of Macronet MN-100	21.6	[33]
Orange bagass	3.73	[34]
Peanut shells-derived activated carbons	50	[28]
Natural Albanian clays	1.956	[35]
Coconut shell-based activated carbon	10.36	[36]
Bentonite clays	5	[37]
60% ZIF-8@Lignin	324.6	Present study

Antimicrobial study

The prepared samples (Lignin, 20%ZIF-8@Lignin, 40%ZIF-8@Lignin, and 60%ZIF-8@Lignin) were tested against bacterial strains via CFU method. Table 4 shows the sensitivity of prepared samples against different bacterial strains. The purified lignin sample was detected the slightly antimicrobial activity against gram positive, gram negative and unicellular fungi [38]. In addition to, ZIF-8 enhanced the antimicrobial activity as compared to pure lignin. [39]. Moreover, 90% of the antimicrobial activity was observed when the concentration of the ZIF-8 was increased. In addition, the MICs values were confirmed the above assumption that the ZIF-8 addition to lignin was caused by the antimicrobial activity of lignin (figure 10). Finally, the MICs values of 60%ZIF-8@Lignin sample were recorded the highest value at 19 µg/ml for all microbial community. Whereas, the pure lignin MICs were recorded at 59 µg mL^{-1} for all

microbial community. These data are confirmed that the 60%ZIF-8@Lignin considered as broad-spectrum antimicrobial agent.

Table 4. Summary of various bacterial strains exhibited antimicrobial susceptibility as tested using CFU method

Samples	*E. coli*	*S. aureus*	*C. albicans*
Lignin	29±0.98	31±1.11	30±0.89
20%ZIF-8@Lignin	66±1.21	78±1.12	71±1.34
40%ZIF-8@Lignin	79±1.56	84±1.89	89±1.22
60%ZIF-8@Lignin	88±1.73	92±1.66	98±1.59
Streptomycin	72±1.38	56±1.33	NA**
Griseofulvin	NA	NA	81±1.88

*Inhibition %, ** This antibiotic is not applicable for this strain

Conclusion

Herein, variety composites from ZIF-8 and lignin were successfully synthesized using eco-friendly one-step technique at room temperature. Microscopic analysis exhibited that ZIF-8 nanocrystals were grown in lignin solution through in situ technique. Surprising, the addition of lignin to ZIF-8 did not destroy the crystallinity of framework. The prepared composites were investigated to uptake of methomyl insecticide from wastewater. The ZIF@Lignin hybrid nanocomposites showed improvement in the upake capacity in comparison with pure lignin. The optimum condition for methomyl removal from wastewater was pH 7, room temperature, 50 mg composite, 3hours and 100mg /L methomyl. The maximum adsorption capacities of lignin, 20%ZIF-8@Lignin, 40%ZIF-8@Lignin and 60%ZIF-8@Lignin were 130, 168, 220 and 324 mg g^{-1}, respectively. The pseudo-second order could well describe the process of adsorbing methomyl on all ZIF-8@Lignin composites. High adsorption uptake of ZIF-8@Lignin composite to remove methomyl from wastewater indicates the great potential of the prepared composites in environmental fields. Additionally, the ZIF-8@Lignin at concentration at 60% was performed as broad spectrum antimicrobial agent.

Declarations

Data Availability

All data generated or analyzed during this study are included in this article

Conflict of interest

The author declare that no conflict of interest for this study

References

1. Karr JR, Dudley DR. Ecological perspective on water quality goals. Environmental management. 1981,5:55-68.
2. Eshra E. Toxicity of methomyl, copper hydroxide and urea fertilizer on some land snails. Annals of Agricultural Sciences. 2014,59:281-4.
3. Jiao G-J, Ma J, Li Y, Jin D, Guo Y, Zhou J, et al. Enhanced adsorption activity for phosphate removal by functional lignin-derived carbon-based adsorbent: Optimization, performance and evaluation. Science of The Total Environment. 2021,761:143217.
4. Wang C, Kelley SS, Venditti RA. Lignin-based thermoplastic materials. ChemSusChem. 2016,9:770-83.
5. Deng Y, Zhao H, Qian Y, Lü L, Wang B, Qiu X. Hollow lignin azo colloids encapsulated avermectin with high anti-photolysis and controlled release performance. Industrial Crops and Products. 2016,87:191-7.
6. Zong E, Huang G, Liu X, Lei W, Jiang S, Ma Z, et al. A lignin-based nano-adsorbent for superfast and highly selective removal of phosphate. Journal of Materials Chemistry A. 2018,6:9971-83.
7. Huang G, Wang D, Ma S, Chen J, Jiang L, Wang P. A new, low-cost adsorbent: Preparation, characterization, and adsorption behavior of Pb (II) and Cu (II). Journal of colloid and interface science. 2015,445:294-302.
8. Mondol MH, Jhung SH. Adsorptive removal of pesticides from water with metal-organic framework-based materials. Chemical Engineering Journal. 2021:129688.
9. Jung BK, Hasan Z, Jhung SH. Adsorptive removal of 2, 4-dichlorophenoxyacetic acid (2, 4-D) from water with a metal–organic framework. Chemical engineering journal. 2013,234:99-105.
10. Abdelhameed R, Abdel-Gawad H, Silva C, Rocha J, Hegazi B, Silva A. Kinetic and equilibrium studies on the removal of 14 C-ethion residues from wastewater by copper-based metal–organic framework. International Journal of Environmental Science and Technology. 2018,15:2283-94.
11. Abdelhameed RM, Taha M, Abdel-Gawad H, Mahdy F, Hegazi B. Zeolitic imidazolate frameworks: Experimental and molecular simulation studies for efficient capture of pesticides from wastewater. Journal of Environmental Chemical Engineering. 2019,7:103499.
12. Jamali A, Shemirani F, Morsali A. A comparative study of adsorption and removal of organophosphorus insecticides from aqueous solution by Zr-based MOFs. Journal of Industrial and Engineering Chemistry. 2019,80:83-92.
13. Abdelhameed RM, Taha M, Abdel-Gawad H, Hegazi B. Amino-functionalized Al-MIL-53 for dimethoate pesticide removal from wastewater and their intermolecular interactions. Journal of Molecular Liquids. 2021,327:114852.

14. Abdelhameed RM, Abdel-Gawad H, Elshahat M, Emam HE. Cu–BTC@ cotton composite: design and removal of ethion insecticide from water. Rsc Advances. 2016,6:42324-33.
15. Lu Z-H, Senosy IA, Zhou D-D, Yang Z-H, Guo H-M, Liu X. Synthesis and adsorption properties investigation of Fe3O4@ ZnAl-LDH@ MIL-53 (Al) for azole fungicides removal from environmental water. Separation and Purification Technology. 2021,276:119282.
16. Senosy IA, Lu Z-H, Abdelrahman TM, Yang M-NO, Guo H-M, Yang Z-H, et al. The post-modification of magnetic metal–organic frameworks with β-cyclodextrin for the efficient removal of fungicides from environmental water. Environmental Science: Nano. 2020,7:2087-101.
17. Abdelhameed RM, Abdel-Gawad H, Emam HE. Macroporous Cu-MOF@ cellulose acetate membrane serviceable in selective removal of dimethoate pesticide from wastewater. Journal of Environmental Chemical Engineering. 2021,9:105121.
18. Abdelhameed RM, Shaltout AA, Mahmoud MH, Emam HE. Efficient elimination of chlorpyrifos via tailored macroporous membrane based on Al-MOF. Sustainable Materials and Technologies. 2021,29:e00326.
19. Minu K, Jiby KK, Kishore V. Isolation and purification of lignin and silica from the black liquor generated during the production of bioethanol from rice straw. Biomass and Bioenergy. 2012,39:210-7.
20. Hasanin MSJES, Research P. Sustainable hybrid silica extracted from rice husk with polyvinyl alcohol and nicotinic acid as multi adsorbent for textile wastewater treatment. 2020,27:26742-9.
21. Hasanin MS, Moustafa GOJIJoBM. New potential green, bioactive and antimicrobial nanocomposites based on cellulose and amino acid. 2020,144:441-8.
22. Salama A, Hasanin M, Hesemann PJCP. Synthesis and antimicrobial properties of new chitosan derivatives containing guanidinium groups. 2020:116363.
23. Shehabeldine A, Hasanin MJEN, Monitoring, Management. Green synthesis of hydrolyzed starch–chitosan nano-composite as drug delivery system to gram negative bacteria. 2019,12:100252.
24. El-Naggar ME, Hasanin M, Youssef AM, Aldalbahi A, El-Newehy MH, Abdelhameed RMJIJoBM. Hydroxyethyl cellulose/bacterial cellulose cryogel dopped silver@ titanium oxide nanoparticles: Antimicrobial activity and controlled release of Tebuconazole fungicide. 2020,165:1010-21.
25. Gomide RAC, de Oliveira ACS, Rodrigues DAC, de Oliveira CR, de Assis OBG, Dias MV, et al. Development and characterization of lignin microparticles for physical and antioxidant enhancement of biodegradable polymers. Journal of Polymers and the Environment. 2020,28:1326-34.
26. Abdelhameed RM, Abu-Elghait M, El-Shahat M. Hybrid three MOFs composites (ZIF-67@ ZIF-8@ MIL-125-NH2): Enhancement the biological and visible-light photocatalytic activity. Journal of Environmental Chemical Engineering. 2020:104107.
27. Yang G-P, Zhao Y-H, Lu X-L, Gao X-C. Adsorption of methomyl on marine sediments. Colloids and Surfaces A: Physicochemical and Engineering Aspects. 2005,264:179-86.
28. Akl M, Youssef A, Hassan A, Maher H. Synthesis, characterization and evaluation of peanut shells-derived activated carbons for removal of methomyl from aqueous solutions. J Environ Anal Toxicol.

2016,6:2161-0525.1000352.
29. Chang C-F, Chang C-Y, Hsu K-E, Lee S-C, Höll W. Adsorptive removal of the pesticide methomyl using hypercrosslinked polymers. Journal of hazardous materials. 2008,155:295-304.
30. El-Geundi M, Nassar M, Farrag T, Ahmed M. Removal of an insecticide (methomyl) from aqueous solutions using natural clay. Alexandria Engineering Journal. 2012,51:11-8.
31. El-Geundi M, Nassar M, Farrag T, Ahmed M. Methomyl adsorption onto Cotton Stalks Activated Carbon (CSAC): equilibrium and process design. Procedia Environmental Sciences. 2013,17:630-9.
32. Fathy NA, Attia AA, Hegazi B. Nanostructured activated carbon xerogels for removal of methomyl pesticide. Desalination and water treatment. 2016,57:9957-70.
33. Chang C-F, Chang C-Y, Hsu K-E, Chiang P. Removal of methomyl pesticide by adsorption using novel hypercrosslinked polymer of macronet MN-100. Journal of the Chinese Institute of Environmental Engineering. 2008,17:311-8.
34. Zimmer TR, Silva JM, de Aquino Rocha DH, Teles HL, Barbosa DS, Freitas FF, et al. Removal of the pesticide methomyl contained in simulated effluent from equipment washing by adsorption in residual orange bagasse. Research, Society and Development. 2020,9:e3569118528-e.
35. Xhaxhiu K, Prifti E, Zitka O. A case study of methomyl removal from aqueous solutions by four natural Albanian clays. Remediation Journal. 2020,30:89-100.
36. Tañala FNA. The effect of surface modification of coconut shell-based activated carbon on methomyl adsorption. 2011.
37. León H, Almeida-Naranjo C, Aldás M, Guerrero V. Methomyl removal from synthetic water using natural and modified bentonite clays. IOP Conference Series: Earth and Environmental Science: IOP Publishing, 2021. p. 012002.
38. Alzagameem A, Klein SE, Bergs M, Do XT, Korte I, Dohlen S, et al. Antimicrobial activity of lignin and lignin-derived cellulose and chitosan composites against selected pathogenic and spoilage microorganisms. 2019,11:670.
39. Taheri M, Ashok D, Sen T, Enge TG, Verma NK, Tricoli A, et al. Stability of ZIF-8 nanopowders in bacterial culture media and its implication for antibacterial properties. Chemical Engineering Journal. 2021,413:127511.

Figures

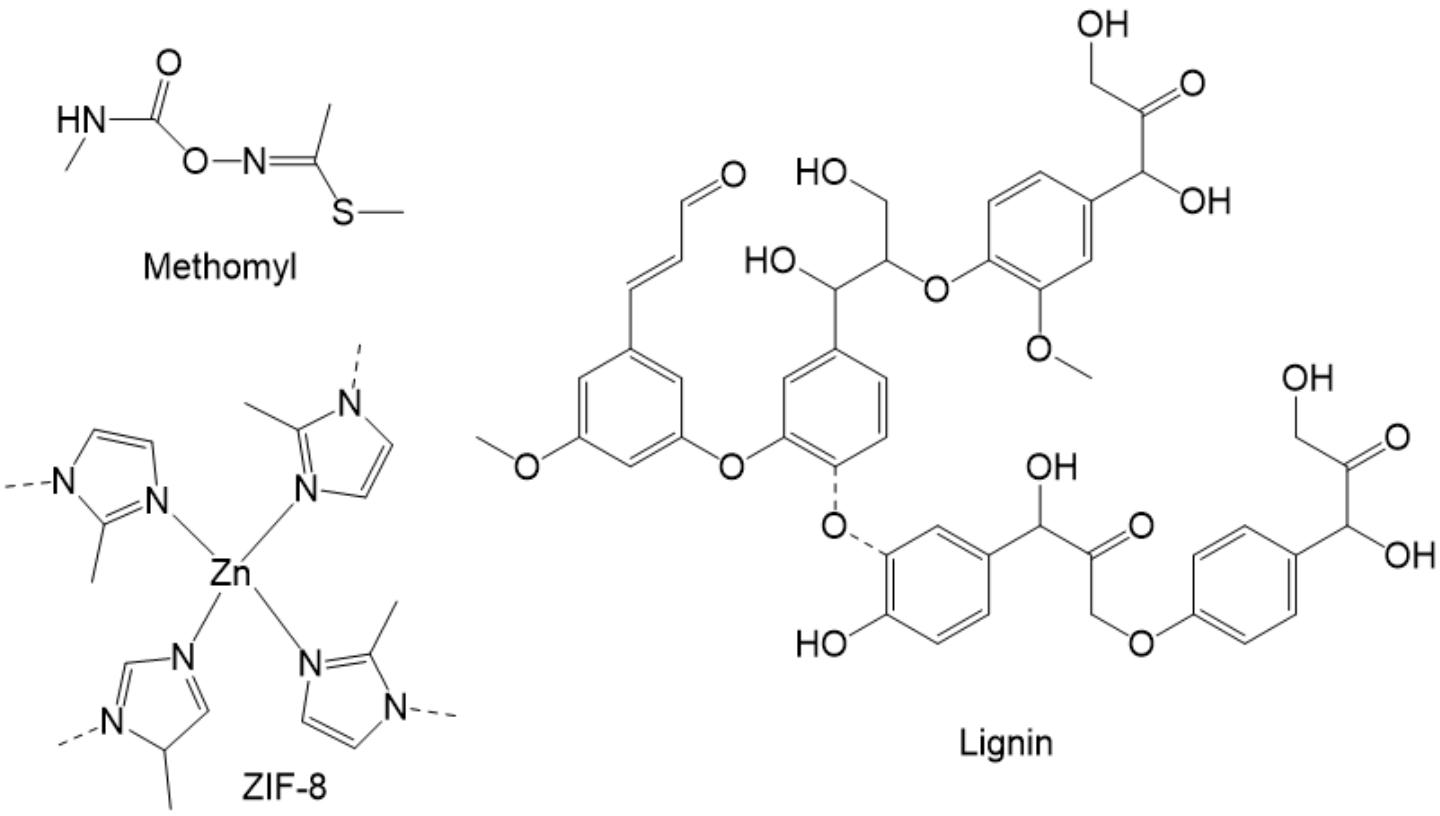


Figure 1

chemical composition of adsorbent and adsorbate.

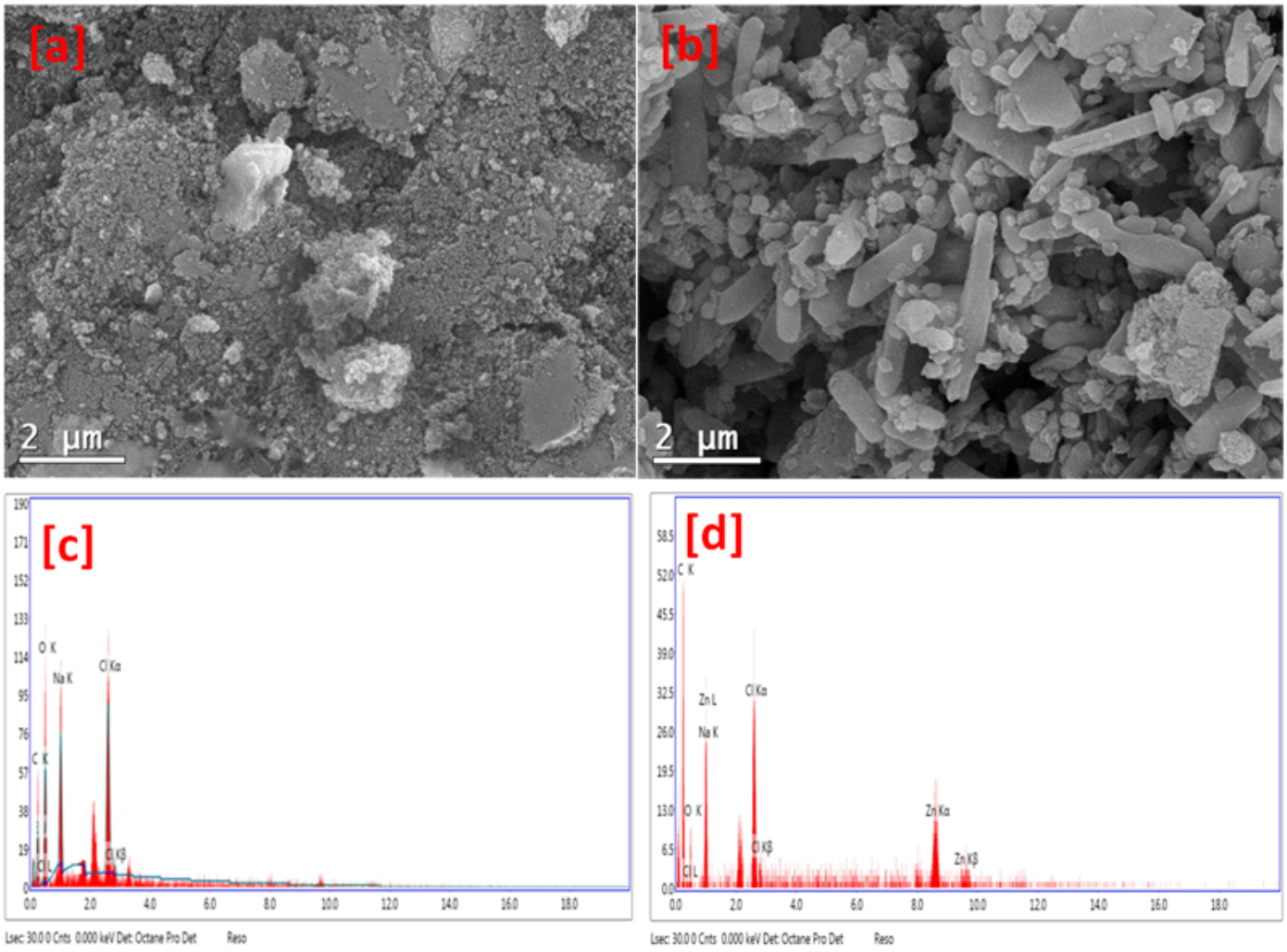


Figure 2

Scanning electron microscopy (SEM) of (a) Lignin, (b) 60% ZIF-8@Lignin, (c) EDX of Lignin, and (d) EDX of 60% ZIF-8@Lignin

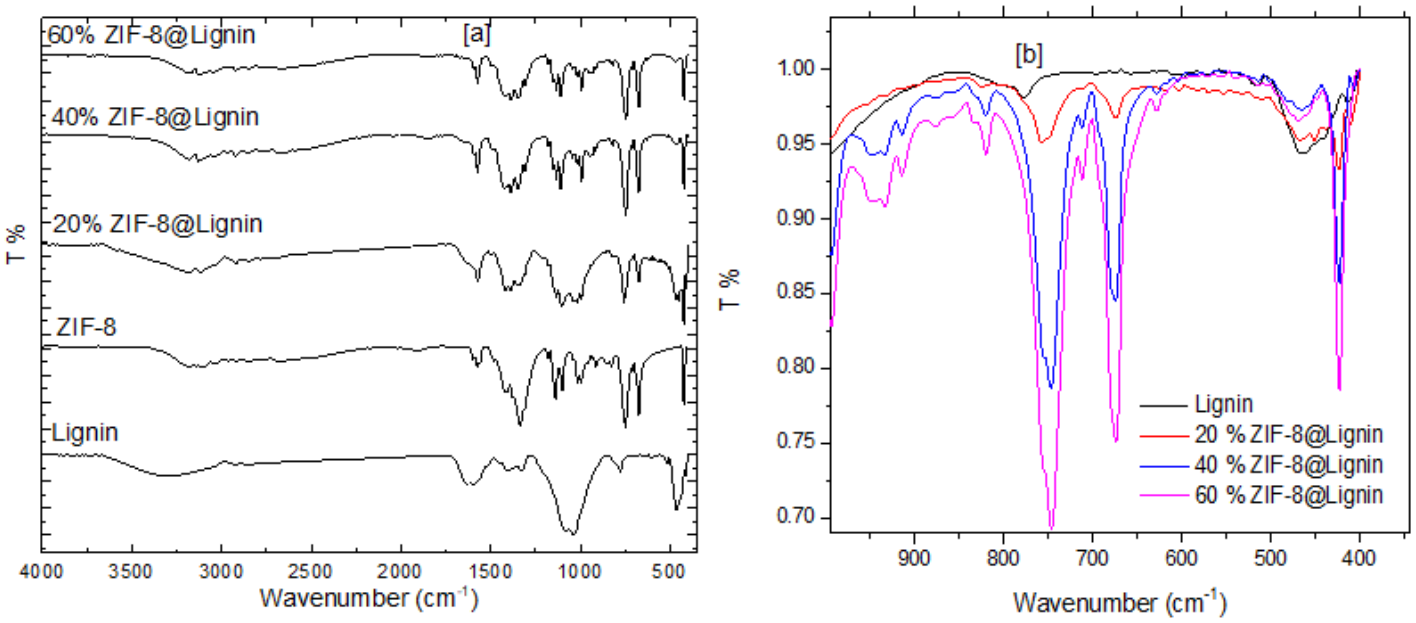


Figure 3

FTIR of [a] Lignin, ZIF-8, 20% ZIF-8@Lignin, 40% ZIF-8@Lignin and 60% ZIF-8@Lignin, [b] FTIR magnification scale for Lignin, 20% ZIF-8@Lignin, 40% ZIF-8@Lignin and 60% ZIF-8@Lignin

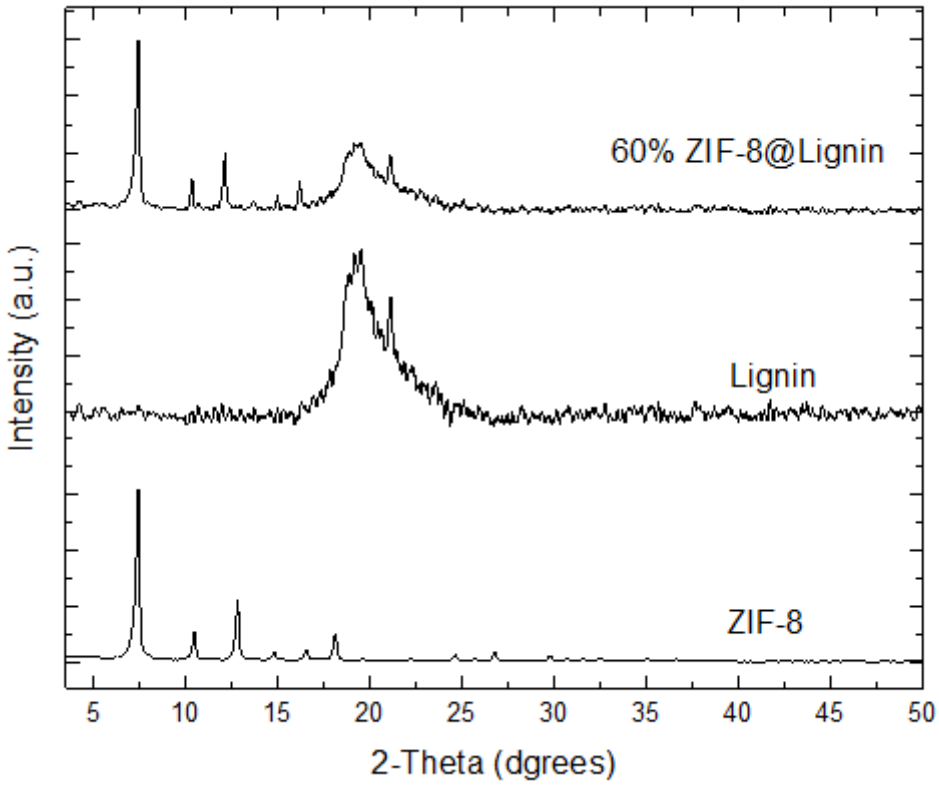


Figure 4

XRD patterns of ZIF-8, Lignin and 60% ZIF-8@Lignin

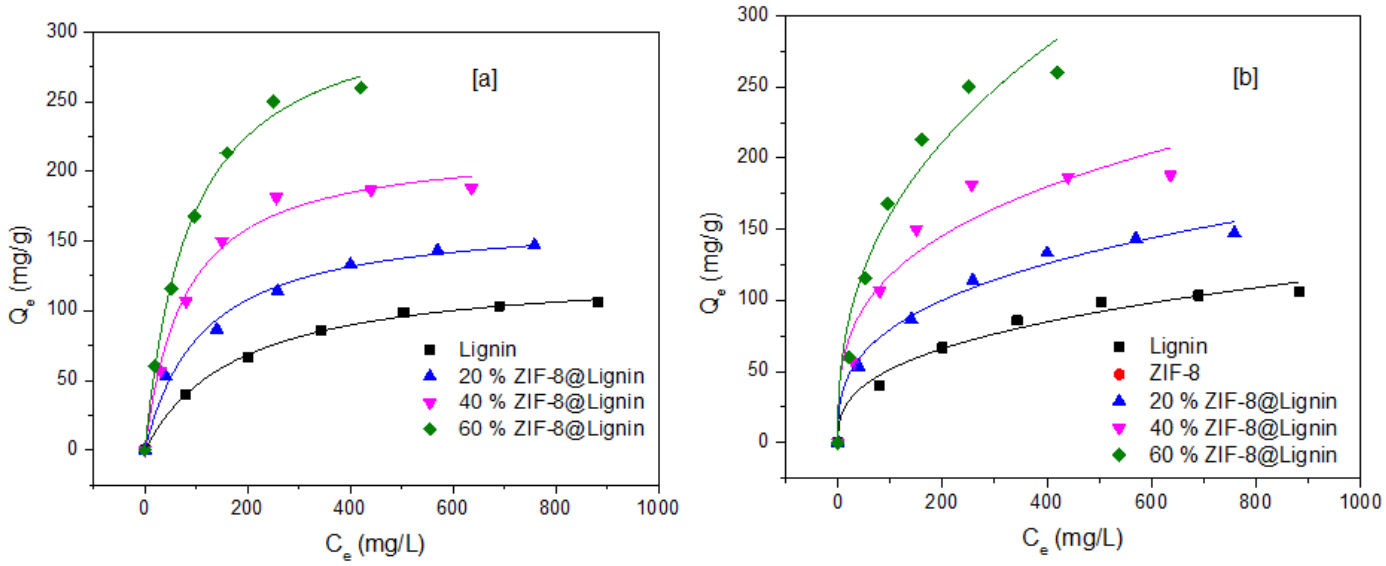


Figure 5

Adsorption isotherm of methomyl onto Lignin, ZIF-8@Lignin (20, 40 and 60%), [a] Langmuir model and [b] Freundlich model

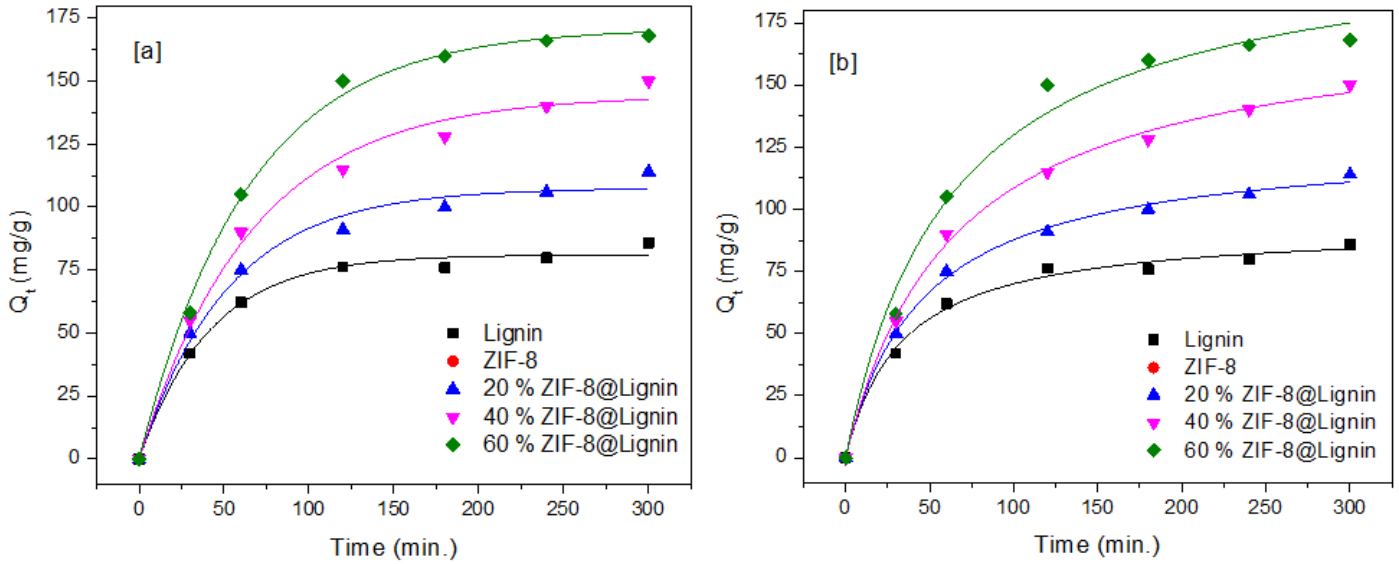


Figure 6

Adsorption kinetics of methomyl onto Lignin, ZIF-8@Lignin (20, 40 and 60%), [a] pseudo first order [b] pseudo-second order.

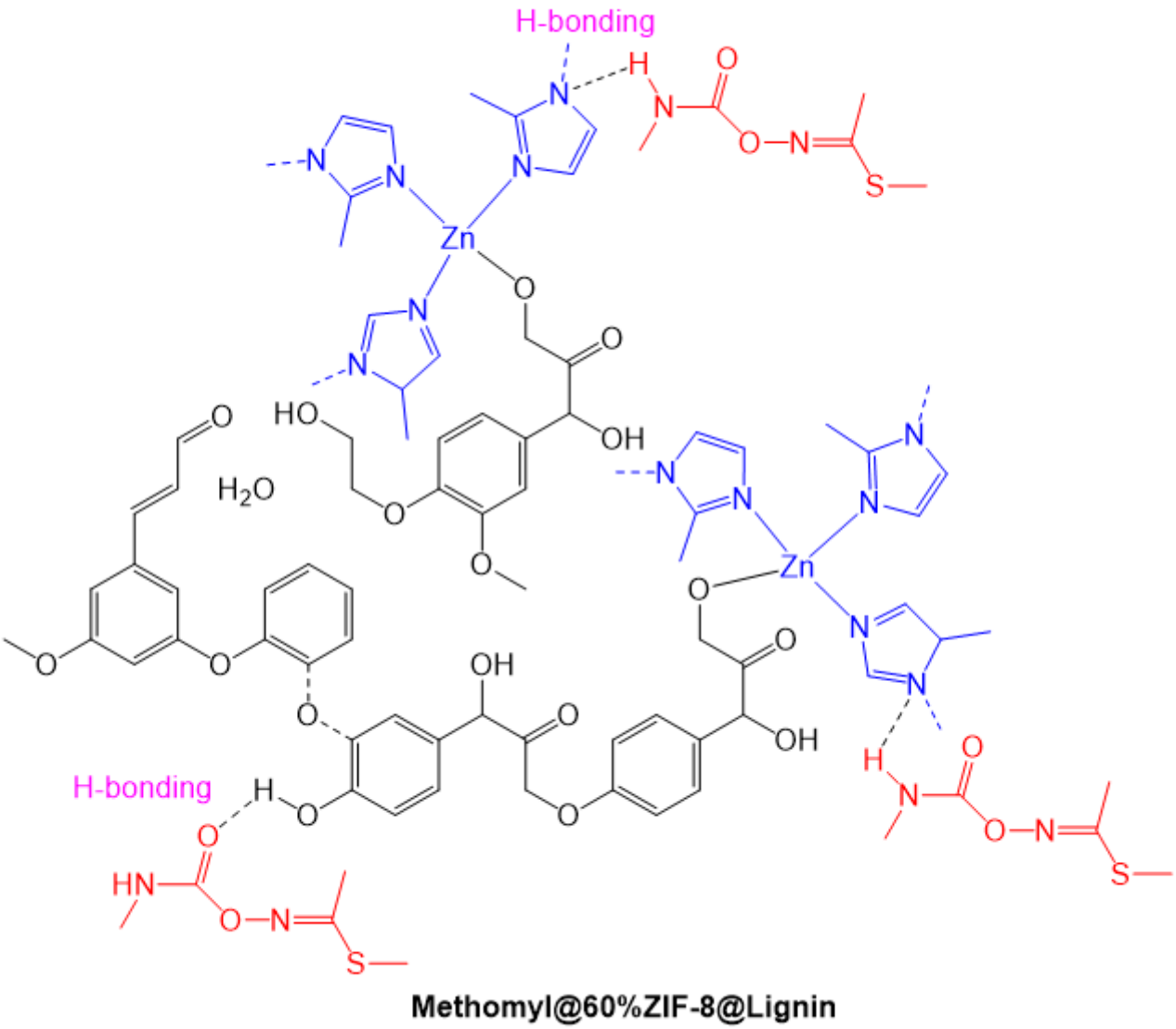


Figure 7

Proposed mechanism for adsorption of methomyl onto 60% ZIF-8@Lignin

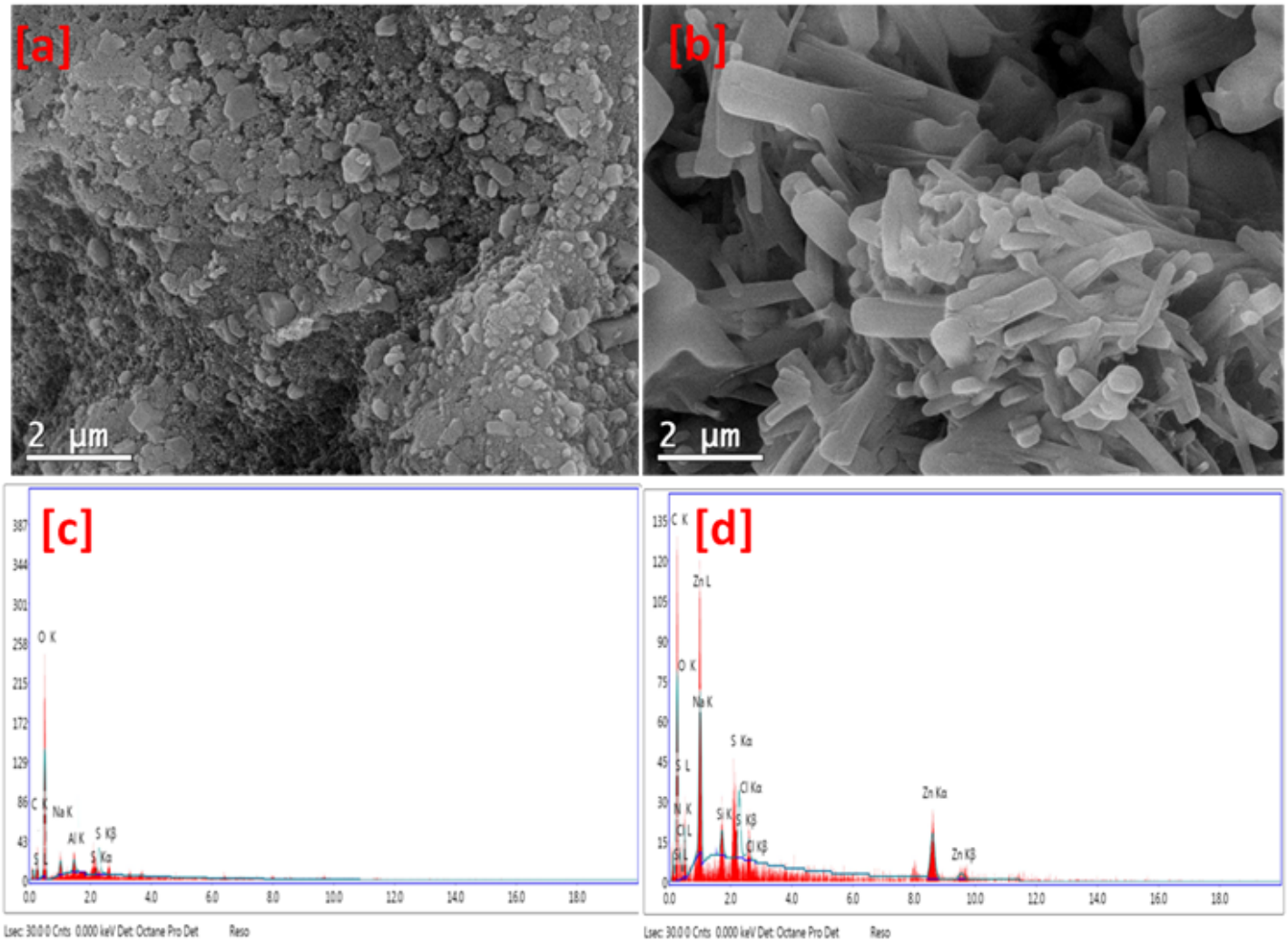


Figure 8

Scanning electron microscopy (SEM) of (a) methomyl adsorbed Lignin, (b) methomyl adsorbed 60% ZIF-8@Lignin, (c) EDX of methomyl adsorbed Lignin, and (d) EDX of methomyl adsorbed 60% ZIF-8@Lignin.

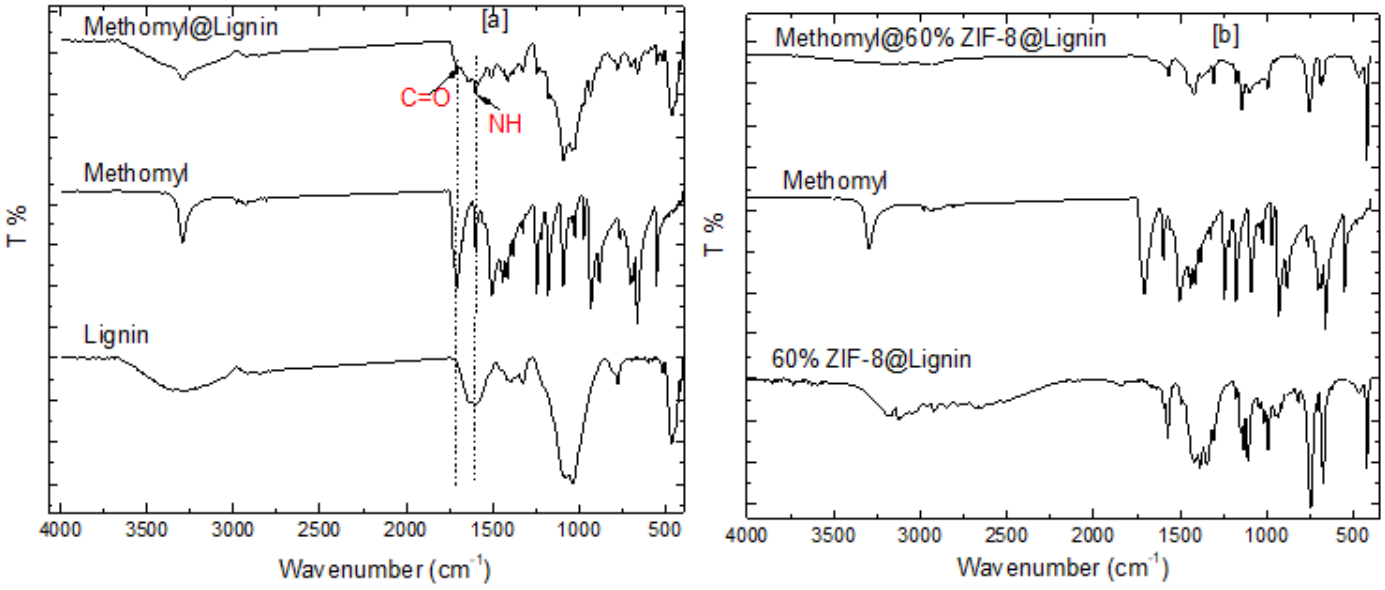


Figure 9

FTIR of (a) Lignin, Methomyl and Methomyl adsorbed Lignin, (b) 60%ZIF-8@Lignin, methomyl and methomyl adsorbed 60% ZIF-8@Lignin.

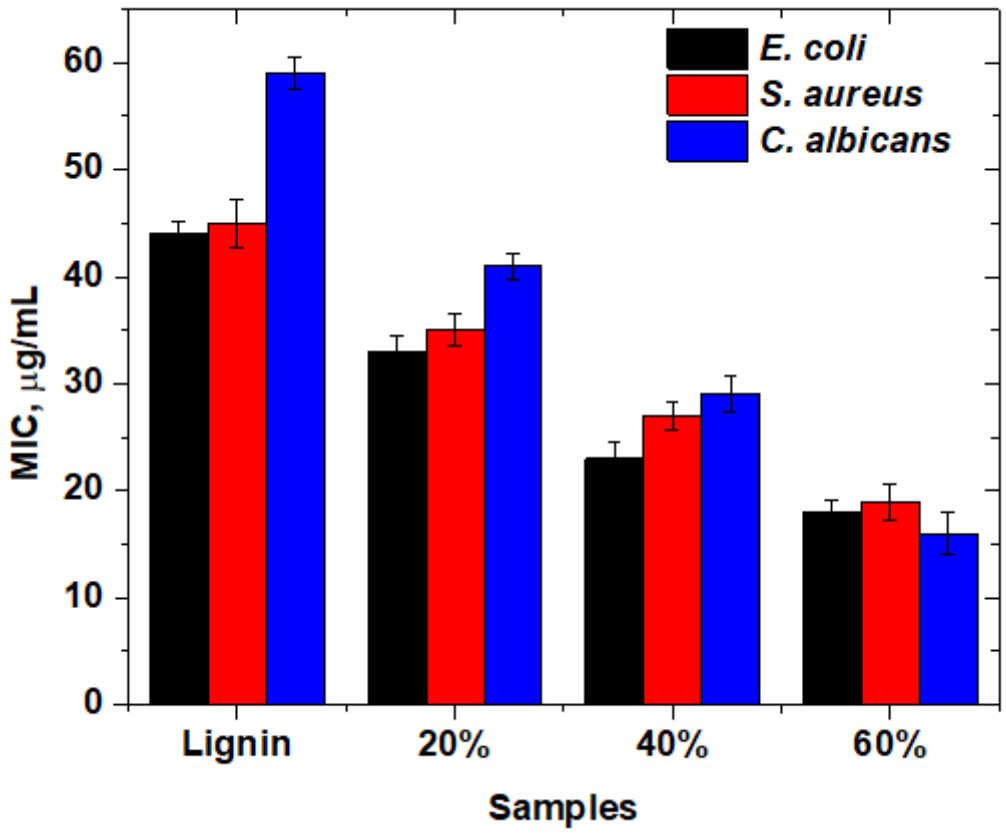


Figure 10

MICs of tested samples